Computational Toxicology 12 (2019) 100091

Contents lists available at ScienceDirect

Computational Toxicology

journal homepage: www.elsevier.com/locate/comtox

In silico site-directed mutagenesis of the *Daphnia magna* ecdysone receptor identifies critical amino acids for species-specific and inter-species differences in agonist binding

Linn M. Evenseth[a,*], Kurt Kristiansen[a], You Song[b], Knut Erik Tollefsen[b], Ingebrigt Sylte[a]

[a] Molecular Pharmacology and Toxicology, Department of Medical Biology, Faculty of Health Sciences, UiT – The Arctic University of Norway, NO-9037 Tromsø, Norway
[b] Section for Environmental Toxicology, Norwegian Institute for Water Research (NIVA), Gaustadalléen 21, N-0349 Oslo, Norway

ARTICLE INFO

Keywords:
Ecdysone receptor
Daphnia magna
Homology modeling
Agonist binding pocket
In silico mutagenicity
MM-GBSA calculations

ABSTRACT

Molting is an essential process in the life cycle of arthropods and is regulated by complex neuroendocrine pathways where activation of the ecdysone receptor (EcR) plays a major role. The EcR forms a non-covalent heterodimer with the ultraspiracle protein (USP) when activated by endogenous ecdysteroids, but can also be activated by several insecticides and other environmental chemicals. Environmental release of exogenous chemicals may thus represent a risk to non-target species due to phylogenetic conservation of the EcR in arthropods. In the present study, structural analysis and homology models of the EcR from the freshwater crustacean *Daphnia magna* were used to characterise the agonist binding pocket and identify amino acids responsible for differences in agonist binding between arthropod species. The analysis showed that the binding pockets of steroidal and non-steroidal agonists are partly overlapping, and the phylogenetically conserved Thr59 is a key residue for binding both types of agonists. *In silico* site-directed mutagenesis and MM-GBSA dG calculations revealed that Cys100 (*D. magna* numbering) is a structural determinant for cross species affinities. Other determinants are Val129 for both types of agonists, Thr132 for steroidal agonists and Asp134 for non-steroidal agonists. The present results can be used to predict cross species sensitivity for EcR agonists, and shows that homology modelling and affinity predictions may contribute to identifying susceptible species for EcR-mediated endocrine disruption.

1. Introduction

Endocrine disrupting chemicals (EDCs) are natural or synthetic compounds that interfere with endogenous endocrine processes such as hormone biosynthesis, metabolism, transport or biological function [1,2]. The EDCs may resemble the structural and chemical properties of endogenous hormones, which make them capable of binding to hormone receptors, and activate or inhibit downstream endocrine processes. The functional outcome of exposure to EDCs is often associated with disruption of growth, development or reproduction [3,4]. These features are highly favourable when the compounds are used as pesticides to control pest populations, but unfortunately they are not always species-specific and may thereby impact non-target species to cause ecological and economic impact [5].

The ecdysone receptor (EcR) is an arthropod nuclear ecdysteroid hormone-dependent receptor, and a molecular target for many EDCs that structurally resemble their endogenous ligands (ecdysteroids). The receptor is a ligand-activated transcription factor that regulates the expression of genes essential for arthropod molting, metamorphosis and reproduction, and is considered an ortholog of the mammalian farnesoid X receptor (FXR) [6]. The EcR is a functional heterodimer, where binding of an endogenous or exogenous ligand to the ligand binding domain (LBD) induces a conformational change enabling dimerization to the ultraspiracle protein (USP). The USP contains a DNA-binding domain (DBD) that allows the dimer to induce gene expression and activate downstream biological processes [7].

Abbreviations: EDCs, endocrine disrupting chemicals; EcR, the ecdysone receptor; FXR, mammalian farnesoid X receptor; LBD, ligand binding domain; DBD, DNA-binding domain; USP, ultraspiracle protein; LBP, ligand binding pocket; AOPs, Adverse Outcome Pathways; KE, key events; MIE, molecular initiating event; AO, adverse outcome; IATA, Integrated Approaches to Testing and Assessment; ROC, Receiver Operating Characteristic; BEDROC, Boltzmann-enhanced discrimination of ROC; AUC, area under the curve; 20E, 20-hydroxyecdysone; Pon A, ponasterone A; MM-GBSA, molecular mechanics Generalized Born Surface area continuum solvation

* Corresponding Author.
E-mail address: linn.evenseth@uit.no (L.M. Evenseth).

https://doi.org/10.1016/j.comtox.2019.100091
Received 19 September 2018; Received in revised form 20 May 2019; Accepted 3 June 2019
Available online 04 June 2019

The usage of EcR agonists as pesticides in agriculture is widespread, which has been demonstrated to be associated with disruption of normal molting and potentially interfere with normal population dynamics of non-target arthropod species (See review by Song et al., 2017a). After the release of X-ray crystal structures of the EcR from various species, it was discovered that the receptor has two partially overlapping ligand binding pockets (LBP), which distinguishes between structural characteristics of steroidal and non-steroidal agonists [8–10]. The amino acid sequences of the EcR are highly conserved across arthropod species, but the EcR ligands display taxon selectivity, most likely caused by small differences in the LBP amino acid sequences between taxa [8,11].

Characterisation of the EcR and the EcR LBP has largely been focusing on insects due to the need for developing effective insecticides with high specificity. The knowledge of the EcR and EcR binding for other arthropods is still limited, albeit the function of the EcR is highly conserved across arthropods. The water flea *Daphnia Magna (D. magna),* a freshwater cladoceran crustacean being a key primary consumer and a significant component of the aquatic food chain, has emerged as a good crustacean model due to the availability of a sequenced genome, well-characterised biology, availability of standardised experimental protocols and high ecological relevance [12]. Recent efforts to study EDC-induced responses in this and other arthropod species has led to the development of Adverse Outcome Pathways (AOPs) where interference with the EcR function and down-stream molecular events leading to molting disruption were identified as the main toxicity pathway [13–15]. The AOPs, which portray and evaluate available data on the molecular initiating event (MIE) and the triggering of a series of key events (KE) that ultimately leads to an adverse outcome (AO) [13,16–19], rely on experimental and computational evidence to define both the taxonomic and chemical applicability domains. Identification of putative arthropod EDCs and target conservation (i.e. receptors) across species are therefore considered instrumental to predict cross species effects and assess the potential risk to non-target species. Effort to develop *in silico* approaches that can rapidly and cost-efficiently identify and prioritise EDCs for further research and regulatory efforts is becoming increasingly important and proposed to partner with the AOP framework to support tiered testing strategies in Integrated Approaches to Testing and Assessment (IATA) [20]. Computational approaches, such as homology modelling, *in silico* mutational studies, docking and scoring and quantitative structure-activity relationship (QSAR) can support and expand the information required for IATAs and assist developing more quantitative prediction models such as quantitative AOPs (qAOPs) [21].

In the present study, we are using a combination of amino acid sequence analysis, homology modelling and calculations of the free energy of binding to study the interactions of agonists with the EcR in *D. magna* and assess the transferability of the binding data to EcR from other arthropods using *in silico* based site-directed mutagenesis.

2. Methods

2.1. Software

Construction and refinement of homology models were performed with MODELLER version 9.17. Evaluation of the models by docking, scoring, Prime/MM-GBSA dG calculations and statistical evaluations by Area Under the Curve (AUC) and the Boltzmann-enhanced discrimination of ROC (BEDROC) scorings were performed with the Schrödinger software version 17.4 [22].

2.2. Structural analysis of EcR-agonist binding patterns

Six available crystal structures of the EcR from different species co-crystalized with different steroidal and non-steroidal agonists (Table 1) were analysed. Amino acids within the binding pockets of steroidal and non-steroidal agonists, and their interaction patterns (hydrogen bonds, hydrophobic- and electrostatic interactions) with co-crystallized agonists were identified. Amino acids within 6 Å from the co-crystallized agonists were considered as relevant for facilitating binding, and considered as the LBP.

Table 1
The crystal structures selected for visual inspection and comparison of bonding patterns in the pocket of steroid like agonists and non-steroid like agonists. The table lists the protein databank (PDB) ID with structural resolution, specie and annotation of co-crystalized agonist.

PDB ID	Resolution (Å)	Complex Agonist	Ligand Structure	Species
3IXP	2.85	BYI08346	Non-steroid	*Helicoverpa armigera*
1R20	3.0	BYI06830	Non-steroid	*Heliothis virescens*
2R40	2.4	20E	Steroid	*Heliothis virescens*
1Z5X	3.07	Ponasterone A	Steroid	*Bemisia tabaci*
2NXX	2.75	Ponasterone A	Steroid	*Tribolium castaneum*
4OZR	2.7	Metylene lactam	Non-steroid	*Bovicola ovis*

2.3. Construction of two agonist datasets

The EcR is highly flexible and adapts the chemical structure of both steroidal and non-steroidal agonists. Two different compound datasets were therefore generated, one with steroidal agonists and one with non-steroidal agonists [10]. Except for 20-hydroxyecdysone (20E) and ponasterone A (Pon A), experimental binding data for the steroidal agonists targeting the *D. magna* EcR was not identified in available databases nor in the literature, but binding data for *D. melanogaster* EcR agonists with a number of steroidal structures was identified. The amino acid sequence identity between the EcR LBD of *D. melanogaster* and *D. magna* was calculated to be > 60% [23]. Nine *D. melanogaster* steroidal agonists were considered active (IC_{50} < 1000 nM) and used in our studies.

Valid experimental binding data of non-steroidal agonists towards *D. magna* EcR was not identified in public databases such as ChEMBL (https://www.ebi.ac.uk/chembl/, accessed august 2017). Non-steroidal EcR agonists for our calculations were therefore selected based on experimental data for other arthropod species (Table 2). A total of 20 non-steroidal agonists (IC_{50} < 1000 nM) were selected for studying the LBP of non-steroidal agonists in the homology models.

The DUD-E database [24] was used to generate property-matched assumed non-binders, referred to as decoys, for each active compound in a ratio of 1:200 as previously recommended [25]. Decoys function as negative controls that resemble the active ligands in the physical chemistry, but are topologically dissimilar. All structures were prepared using Schrödinger LigPrep [26] with a target pH of 7.4, retaining specified chiralities and generation of tautomers.

Table 2
The number of non-steroid like agonists tested for the EcR from different species. Some agonists have been tested in multiple species. Twenty non-steroid like agonists were included in our studies.

Specie	#Compound
Nezara viridula	2
Bombyx mori	12
Spodoptera littoralis	8
Heliothis virescence	1
Drosophila melanogaster	13

2.4. Construction of and validation of homology models

The complete amino acid sequence of the *D. magna* EcR LBD was obtained from the Uniprot database [27]. Two templates were identified from the Protein Data Bank (PDB) based on sequence identity with the target (*D. magna* EcR), and used to construct the homology models. The selected templates were the EcR LBD from *Bemisia tabaci* co-crystalized with 20E (PDB id: 1Z5X), and the EcR LBD from *Heliothis virescens* co-crystallized with the non-steroidal agonist BYI06830 (PDB id: 1R20). The MODELLER software was used to generate and refine 100 homology models per template. The software constructs the model in three steps as described by Eswar et al., 2006: (1) Assignment of folds by identification of similarity between templates and target, (2) Sequence alignment of templates and target, and (3) Construction of homology models based on the selected templates. The models were energetically and structurally optimized using the protein preparation wizard in Schrödinger Maestro [22,28–30] with the OPLS3 force field.

The respective agonists and corresponding property-matched decoys were docked in all homology models as previously described [31]. The 100 homology models generated per template were evaluated by their abilities to differentiate active from decoys by employing AUC and BEDROC scoring. BEDROC addresses the "early recognition" problem by weighting the contribution of rank to the final score by using a single parameter called α. After docking of all active compounds and their corresponding decoys, the compounds were ranked according to docking score and an α value of 20 was used to ensure that the contribution to the final BEDROC score came from the first ranked 8% of all docked compounds as recommended by Truchon et al. [26]. The AUC and BEDROC scores were calculated and used to rank and select the best models in combination with visual inspections. Both AUC and BEDROC give scores for the models ranging between 0 and 1, where 1 indicates a perfect model able to recognize and separate all actives from decoys. The models were evaluated based on AUC and BEDROCK scores and the top scoring ones were selected for *in silico* mutagenesis, docking of 20E, Ponasterone A, BYI08346 and BYI06830 and Prime/MM-GBSA calculations.

2.5. Multiple sequence alignment, docking and mutational studies

All available crystal structures of the EcR in the PDB were used for generating a multiple sequence alignment using the Schrödinger Maestro multiple sequence viewer. Amino acid sequences of the EcR LBD from all the species with known EcR agonists considered as active (IC_{50} < 1000 nM) were identified in Uniprot and included in the alignment.

The amino acids within the LBPs from the structural analysis of the X-ray structures were mapped to the other sequences of the alignment using the multiple sequence viewer (MSV) [32]. The sequences were renumbered according to the homology models. All amino acids within the LBP that were different from the query sequence (*D. magna*) contributing to differences in charge, size or polarity in the LBP were used as a reference for *in silico* mutation of the *D. magna* sequence in the selected homology models (Table 3). In this way, the energy contributions to agonist binding caused by species-specific differences in the LBP could be analysed. After inducing mutations, hydrogen bonds were optimised and the protein re-minimized before performing a docking protocol with standard precision (SP) of agonists from known EcR X-ray structures (Table 1). However, methylene lactam was not docked since it was found to destabilize the functional heterodimer in solution [33], indicating putative antagonistic properties. Enhanced sampling of conformer generation and expanded sampling for selection of initial poses (receptor-agonist complex) were used with flexible ligand sampling.

During docking into mutated EcRs using standard precision, new ligand docking poses were included in the stack of docking poses (using Maestro Pose Viewer files) only if Coulomb and Van der Waals (VdW) interaction energies were < 0 kcal/mol and the root mean square deviation (RMSD) were > 0.5 Å from previous poses. This procedure ensures the identification of conformationally different docking poses. The molecular mechanic energies combined with Generalized Born Surface area continuum solvation (MM-GBSA) methods [22] were used to estimate the binding free energy (dG) of the different docking poses in wild type EcR (*D. magna*) and the mutated EcR homology models. The MM-GBSA calculates energies associated with the ligand, receptor and the complex as well as differences in energies associated with strain and binding [34] and approximates the relative free energy of binding (the more negative value, the more favourable is the binding of the ligand to the receptor). This was used to evaluate if the introduced mutation changed the relative affinity of agonists towards the receptor. The highest ranked docking pose in terms of binding free energy was selected as the final and most accurate pose. The relative MM-GBSA dG value calculated for un-mutated receptor (*D. magna*) upon re-docking of steroids (20E and Pon A) and non-steroids (BYI08346 and BYI06830) were used as a threshold to evaluate the effects of the introduced mutations. The percentage change in dG of agonist binding to the mutated receptor relative to the non-mutated was calculated and used to evaluate the introduced mutations and thereby the EcR agonist potential for causing effects in other species.

3. Results

3.1. Evaluation of EcR-agonist binding patterns

The multiple sequence alignments show that the residues in the two LBPs are well conserved between the species included in the alignments, but the X-ray structures show that the LBP for steroidal agonists is different and only partially overlapping with the LBP of non-steroidal agonists (Fig. 1, S1 and S2). The steroidal LBP is slightly bigger than the non-steroidal pocket. In *D. magna* EcR homology models, the volume of the LBP of steroidal LBP is 417.7 $Å^3$, while that of the non-steroidal is 373 $Å^3$. The only structural difference between Pon A and 20E is a hydroxyl group attached to the alkyl side chain of 20E (Fig. 2).

Visual inspection of the three X-ray structures co-crystalized with steroids, Pon A (PDB ID: 1Z5X and 2NXX) [35,36] and 20E (PDB ID: 2R40) [37], revealed that 14-OH, 20-OH and 6-oxo functional groups of the steroids are forming hydrogen bonds with Glu23, Thr59 and Ala114 (Val114 in the structure of *T. castaneum*). In total, up to six different amino acids were participating in hydrogen bonds with the steroids, but except for Glu23, Thr59 and Ala114, the other three varied between the complexes. The X-ray structures indicated that some of the hydroxyl groups present in the steroids function as both hydrogen bonding donors and acceptors.

Investigation of three published X-ray structures of the EcR in complex with agonists of non-steroidal structure (PDB ID: 1R20, 3IXP and 4OZR) [33,38] showed that the number of hydrogen bonds formed between the agonists and the amino acids in the LBP is significantly lower than that of steroidal agonists. BYI08346 form three hydrogen bonds with EcR from *H. armigera*, while BYI06830 form two hydrogen bonds with EcR from *H. virescens*, despite having equal numbers of putative hydrogen bonding donors and acceptors. The X-ray structures show that Thr59 and Tyr124 participate in hydrogen bonding both with BYI08346 and BYI06830.

Interestingly, the X-ray structures indicated that Thr59 was involved in the binding of both steroidal and non-steroidal agonists (Fig. 1) and Thr59 was involved in hydrogen bonds in all X-ray complexes.

3.2. Construction and structural analysis of homology models

One homology model per template was selected based on the BEDROC values, AUC and supported by visual inspection (Table 4). The statistical analysis showed that model number 23 was the most appropriate for the steroidal LBP due to an AUC value of 1 and a BEDROC

Table 3
Amino acids within 5 Å of the agonist in the agonist LBP of known EcR X-ray structures with the corresponding amino acids in EcRs from other species with available agonist data. Only amino acids at positions that are varying between the different species are included in the table. *D. magna* sequence numbering is used. All amino acids significantly different from the *D. magna* sequence was mutated in the *D. magna* homology models.

Species/PDB-code	Binding pocket steroid ligands							Binding pocket non steroid ligands								
Seq. position	23	24	66	100	129	132	222	58	66	100	129	132	133	134	228	231
D. magna	D	Q	T	C	V	T	L	M	T	C	V	T	A	D	L	E
2r40	E	Q	I	V	M	V	Q	M	I	V	M	V	I	E	Q	N
1r20	E	Q	I	V	M	V	Q	M	I	V	M	V	I	E	Q	N
3ixp	E	Q	I	V	M	V	Q	M	I	V	M	V	I	E	Q	N
2nxx	E	H	I	M	M	T	Q	I	I	M	M	T	I	E	Q	E
1z5x	E	H	I	M	M	T	M	I	I	M	M	T	V	E	M	E
4ozr	E	Q	I	M	M	T	L	I	I	M	M	T	V	D	L	E
S.littoralis	E	Q	I	V	M	V	Q	M	I	V	M	V	I	E	Q	N
D.melanogaster	E	Q	I	M	M	N	Q	I	I	M	M	N	I	E	Q	E
N.viridula	E	H	I	M	M	V	Q	I	I	M	M	V	I	E	Q	E
B.mori	E	Q	I	V	M	V	Q	M	I	V	M	V	I	E	Q	N
Mutation	D/E	Q/H	T/I	C/V C/M	V/M	T/N T/V	L/Q	M/I	T/I	C/M C/V	V/M	T/V T/N	A/I	D/E	L/Q	E/N

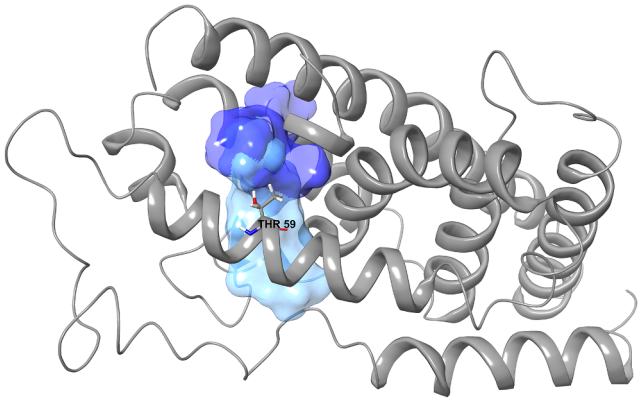

Fig. 1. The EcR of *D. magna* with the binding pocket for steroid like agonists (dark blue mesh) and the binding pocket of non-steroid like agonists (light blue mesh) indicated. These binding pockets are only partially overlapping. Thr59 is positioned in the overlapping area between the binding pockets. In all available X-ray structures, this residue is observed to form hydrogen bonds with bound agonist independent of which pocket they are located within.

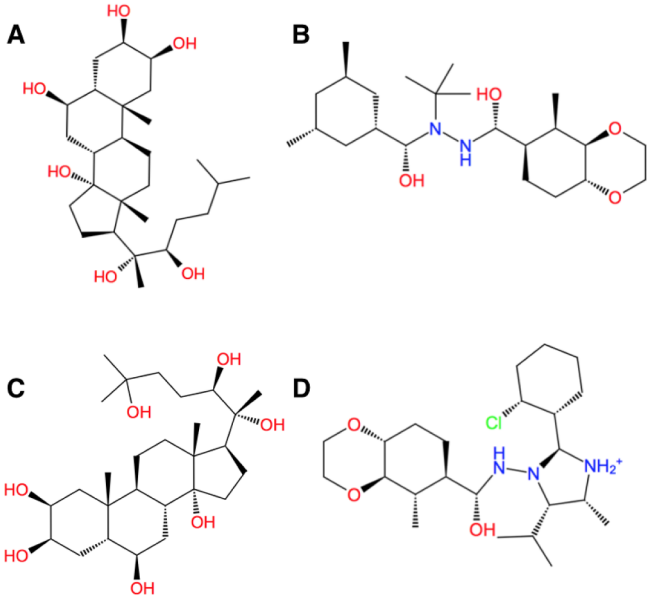

Fig. 2. The structure of the agonists that were docked in the homology models to study the effects of a various mutations. A: Ponasterone A, B: BYI08346, C: 20E, D: BYI06830.

value of 0.994, which indicates a good predictive model, and the model was selected as the homology model to represent the steroidal LBP. Model number 97 with an AUC value of 0.98 and a BEDROC value of 0.8 was selected to represent the non-steroidal LBP. Model 56 also had an AUC of 0.98, but model 97 was selected based on better BEDROCK score (Table 4 and S3).

3.3. Docking and MM-GBSA calculations

A total of 9 mutations were introduced in the steroidal and 11 in the non-steroidal LBP of the *D. magna* EcR homology models based on species differences in key amino acids of the LBP (Table 3). The co-crystalized agonists of the studied X-ray structures were docked in the respective homology models (non-steroids: BYI08346 and BYI06830, steroids: ponasterone A and 20E), such that the non-steroidal agonists were re-docked in 11 models and the steroidal ligands in 9 models. Structural investigation of the LBPs showed that the steroidal LBP and the non-steroidal LBP are different and partly overlapping (Fig. 1 and Fig. 3), and that the steroidal LBP appeared to be more conserved than the LBP for non-steroidal agonists. The dG for the receptor without mutations was calculated to be −109.3 kcal/mol for the binding of Pon A, −108.7 kcal/mol for 20E, −87 kcal/mol for BYI08346 and

Table 4
The 10 top ranked homology models generated from the two templates. The Model numbering was automatically generated by MODELLER. The most optimal models were identified on basis of BEDROC and AUC scores (in bold).

HM steroid	BEDROC (alpha 20)	AUC	HM Non-steroid	BEDROC (alpha 20)	AUC
23	**0.994**	**1.0**	56	0.7	0.98
83	0.906	0.99	**97**	**0.802**	**0.98**
1	0.792	0.98	39	0.613	0.96
10	0.798	0.98	40	0.628	0.95
55	0.799	0.98	44	0.581	0.94
89	0.781	0.98	69	0.514	0.94
95	0.689	0.97	49	0.734	0.93
34	0.691	0.97	15	0.741	0.93
80	0.559	0.96	31	0.761	0.931
70	0.553	0.96	43	0.560	0.931

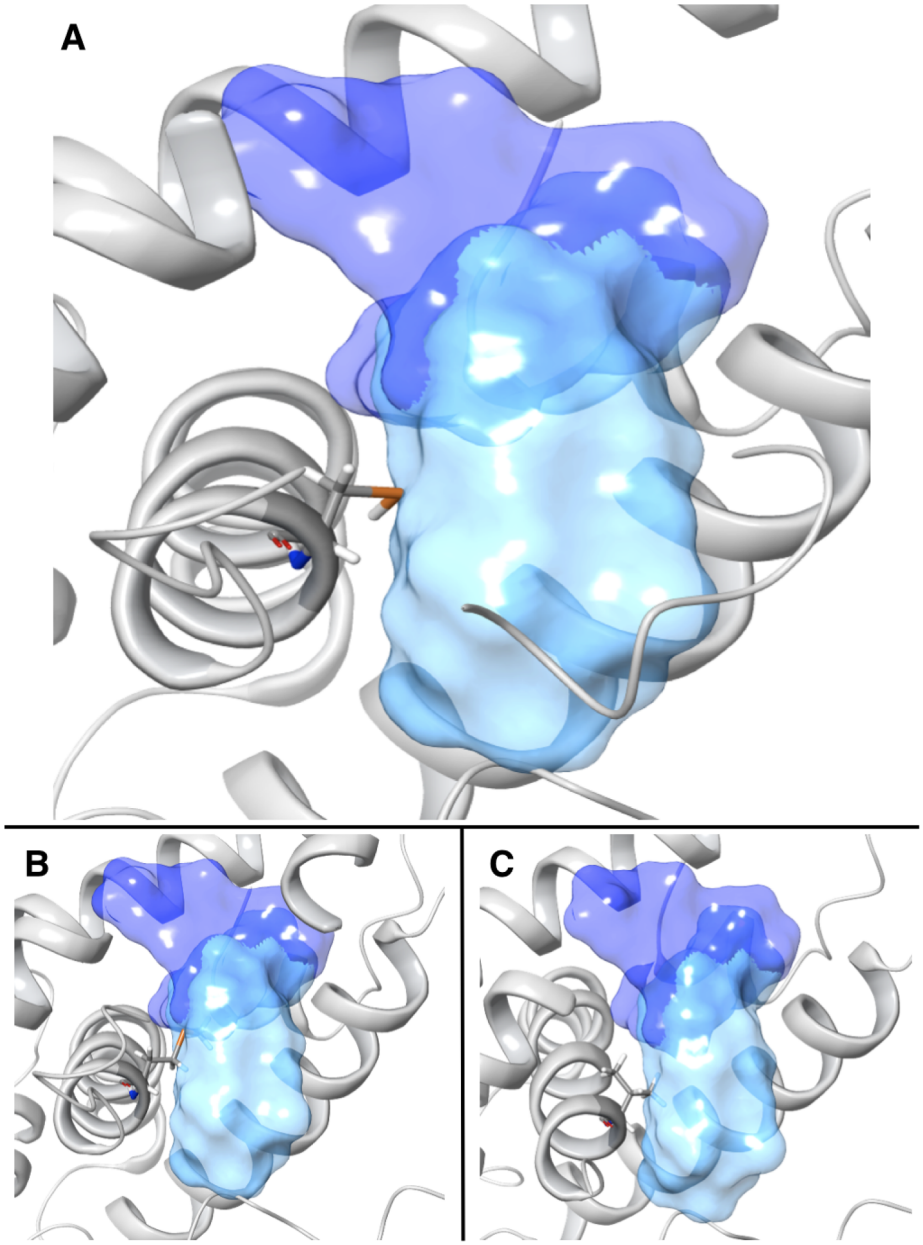

Fig. 3. The binding pocket of steroid like agonists (light blue) and non-steroid like agonists (dark blue) superimposed and displayed in homology model 23 with Cys100 displayed. The position of Cys100 is similar in all the models. A) In the wild type *D. magna* sequence, the polar Cys100 is in very close proximity to the steroid binding pocket without penetrating into the pocket. B) Cys100Met mutation enables Met100 to infiltrate the pocket for steroid like agonists, and is also closer to the binding pocket for non-steroid like agonists. C) Cys100Val mutation enables valine to penetrate the pockets with one of the hydrophobic methyl groups of the side chain.

−86.2 kcal/mol for BYI06830. These values were used as thresholds for evaluating effects of the introduced mutations and thereby assess the putative potential for EcR-mediated effects in other species.

3.4. Mutation in the steroidal binding pocket

The introduced mutations affected the two steroids differently, but the mutations did not dramatically change the free energy associated with steroidal binding. In total, only two of the mutations, Cys100Val and Val129Met, had a clear increase in dG for Pon A to a weaker binding energy, with changes between 16 and 17% compared to the dG of the non-mutated receptor due to change in the interaction pattern (Figs. 4–6). Mutation Cys100Val changed the dG by approximately 7% for 20E, while the Val129Met mutation changed dG with approximately 12% (Figs. 4 and 5). These mutations also had the biggest impact on the binding of 20E of all mutations. The mutation of Cys100Met gave similar results for both ligands, whereas dG for Pon A increased by 5.2% and for 20E with 6.2% into weaker binding than that observed in the non-mutated EcR (Figs. 4 and 5).

Compared with the non-mutated EcR, the mutations Gln24His, Thr132Asn and Lys228Gln all favourably decreased dG with 7.6–10% for 20E (stronger binding than to the non-mutated receptor), but with only 0.3–1.2% increase for Pon A (Fig. 4). The mutation Thr132Val slightly affected Pon A binding compared to the non-mutated receptor, as the decrease in dG was approximately 2%. The decrease in dG for 20E for Thr132Val was into 8.5% stronger binding than in the non-mutated EcR.

The LBP for steroidal agonists in *D. magna* EcR contains an aspartic acid (Asp23) and a threonine (Thr66) that are unique for this species, while the other examined species contains a glutamic acid and an isoleucine at these positions (Table 3). The MM-GBSA calculations showed that the Asp23Glu slightly increased the dG for Pon A (approximately 1.9%), while we saw a decrease (approximately 5%) for 20E, compared to the un-mutated receptor (Fig. 4). The Thr66Ile mutation did not affect dG for Pon A, but decreased the dG for 20E compared to the un-mutated complex giving approximately the same value as seen for the Asp23Glu mutant (Fig. 4).

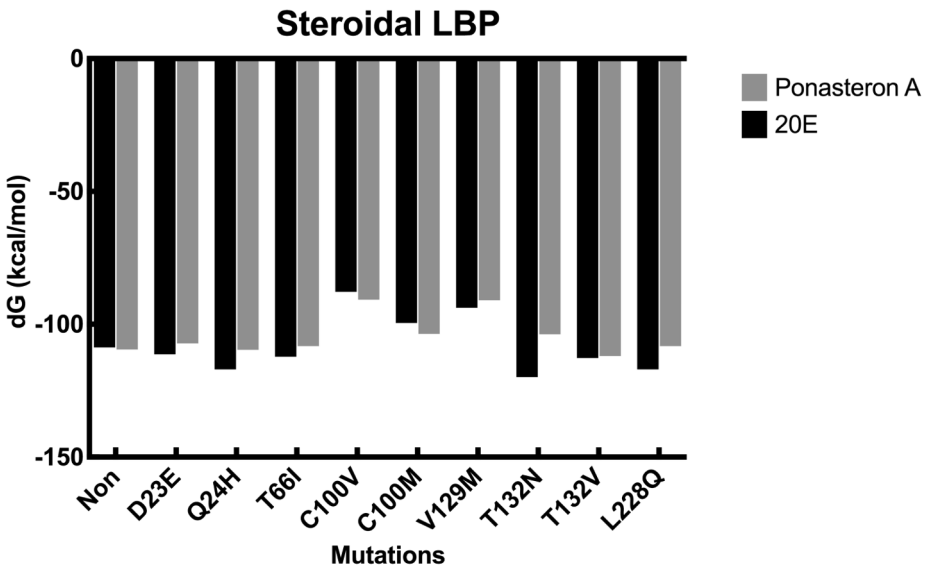

Fig. 4. The calculated differences in free energies upon binding of steroid like agonists for the un-mutated wild type *D. magna* receptor (non) and the different mutated receptors. Gray bars show the free energy changes upon ponasterone A binding, while black bars show the free energy changes upon 20E binding.

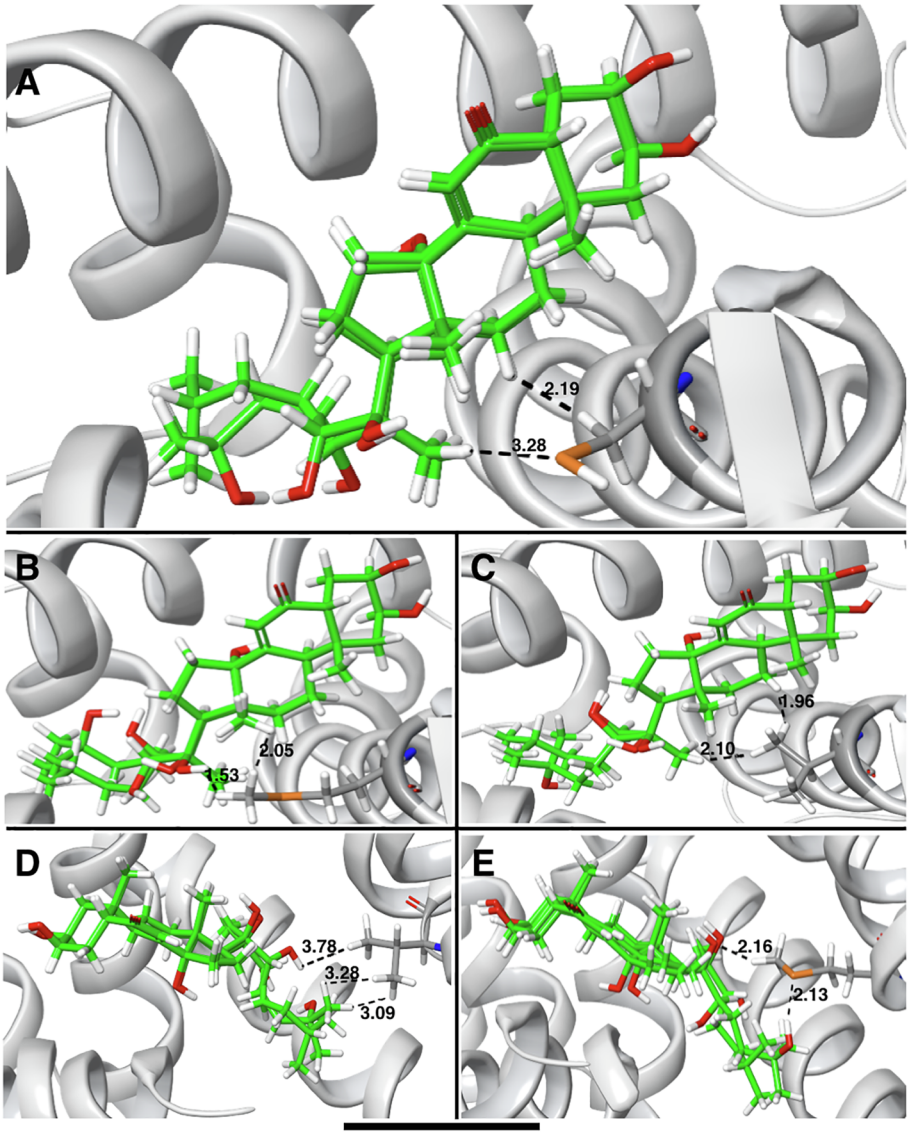

Fig. 5. The binding pocket for steroid like agonists in homology model 23 with ponasterone A and 20E superimposed at their binding sites. A) Cys100 cysteine is positioned 2.19 Å and 3.28 Å to the closest ligand atom in the binding pocket and is stabilized by hydrophobic interactions. B) Cys100Met mutation did not interfere with the binding poses and M100 is stabilizing the ligands due to hydrophobic forces. C) Cys100Val is less favourable since a methyl group of valine enters deeper into the pocket than cysteine and comes in close proximity to the agonists. D) Val129 stabilizes the hydrophobic carbon tail of the steroid like agonists. E) Val129Met mutation induces sterical clashes between the receptor and the steroid like agonists.

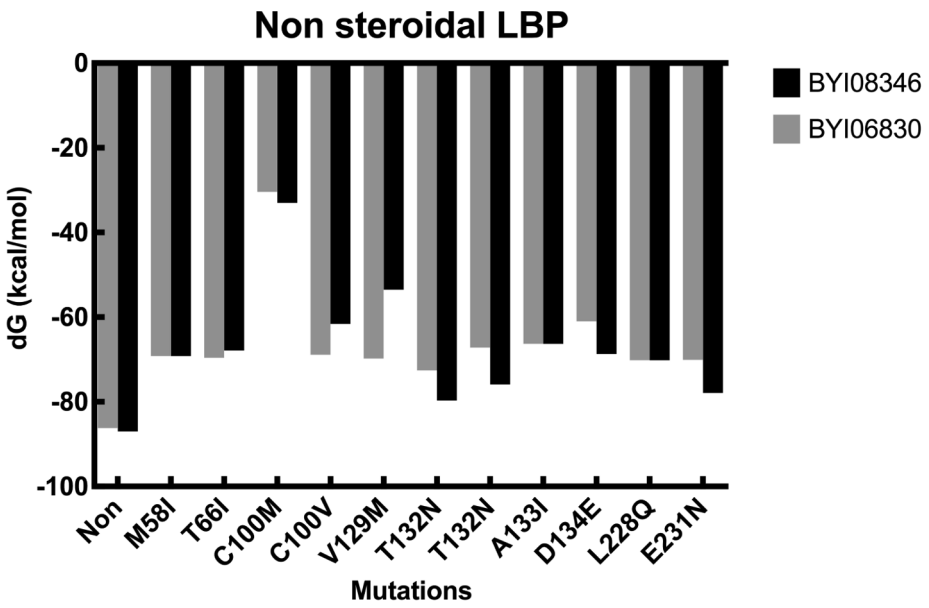

Fig. 6. The calculated differences in free energies upon binding of non-steroid like agonists for the un-mutated wild type *D. magna* receptor (non) and the different mutated receptors. Black bars show the free energy changes upon binding of BYI08346, while gray bars show the free energy change upon binding of BYI06830.

3.5. Mutations in the non-steroidal binding pocket

The Cys100Met mutant increased the dG with approximately 60% for both non-steroidal agonists, likely due to larger sterical interference of methionine with optimal ligand-receptor binding for non-steroids than the cysteine (Figs. 6 and 7). Of all mutations, this mutation gave the most dramatic changes in dG compared with the un-mutated receptor. Changing the cysteine to valine in the same position (Cys100Val) increased the dG with approximately 20% for BYI06830 and 30% for BYI08346 giving weaker interactions than in the non-mutated receptor, due to the shorter hydrophobic chain in the amino acid valine compared to methionine (Figs. 6 and 7).

The Val129Met increased dG with 20% for BYI06830 and 40% for BYI08346 relative to the non-mutated receptor, while the Thr132Val, Thr132Asn and Gln231Asn increased dG by 8–12% for BYI08346 and with 15–22% for BYI06830, respectively.

Thr66 is present in the LBP of both non-steroidal and steroidal agonists. Mutating this residue to an isoleucine (Thr66Ile) increased the dG of non-steroidal agonist binding by approximately 20%, thus giving weaker binding of both the non-steroidal agonists for the Thr66Ile than

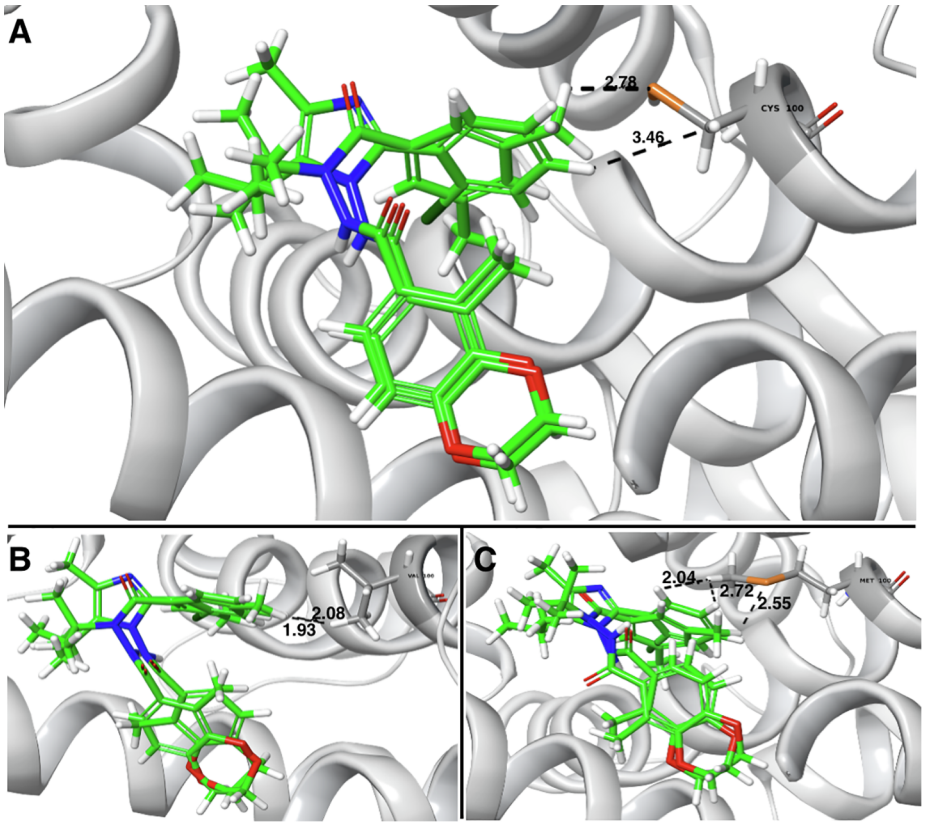

Fig. 7. BYI06830 and BYI08346, superimposed in the binding pocket of homology model 97. A) The side chain of Cys100 in the binding of the wild type receptor forms interactions with the non-steroid like agonists at atomic distances of 2.78 and 3.46 Å, respectively. The side chain of Cys100 is forming hydrogen bonds with a hydrogen in the aromatic ring of BYI06830 and with the methyl group of BYI08346. B) Cys100Val mutation gave similar binding poses, but with the agonists slightly closer to Val100 than Cys100. The atomic distance from the agonists to the closest side chain atom was 1.93 Å for BYI06830 and 2.08 Å for BYI08346. C) The Cys100Met mutation increased the hydrophobicity of the pocket and the agonists are located closer to Met100 than Cys100 at atomic distances of 2.55 Å (BYI08346) and 2.04 Å and 2.72 Å (BYI06830).

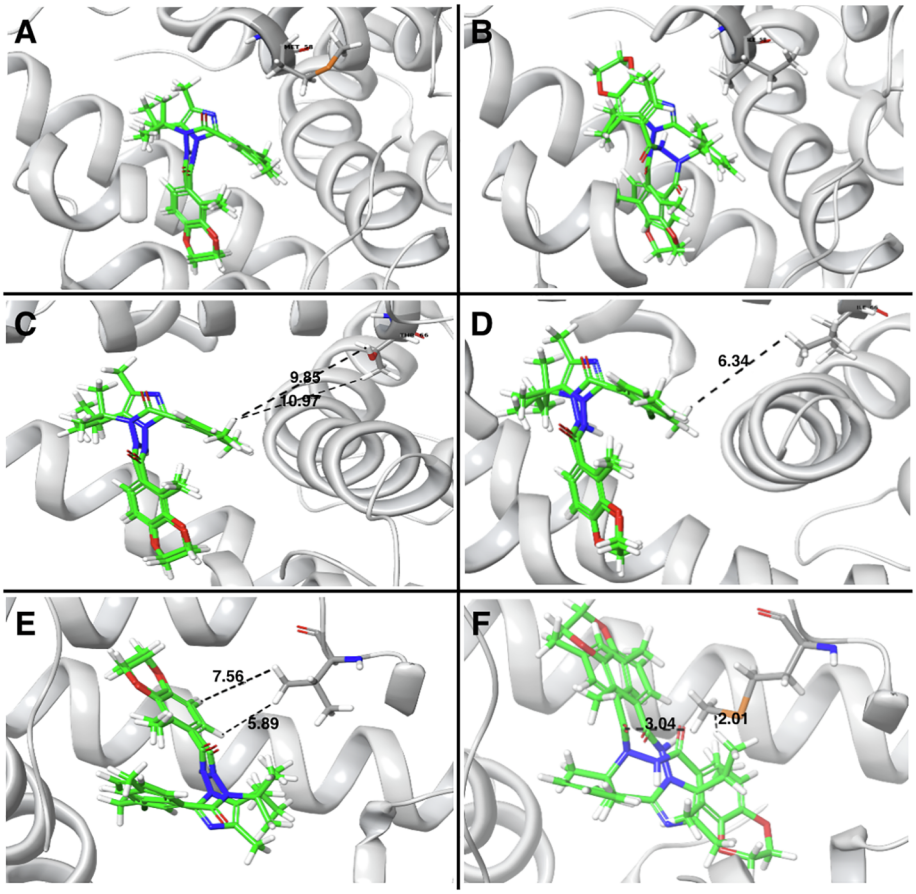

Fig. 8. The binding pocket of non-steroid like agonists in homology model 97 with BYI08346 and BYI06830 superimposed at their binding sites. The agonists are stabilized in the binding pocket by long range hydrophobic forces. A) Met58 (wild type receptor) forms hydrophobic interactions with the non-steroid like agonist. B) The Met58Ile mutation slightly changes the agonist position and decreases the interactions. C) Thr66 located at distances of 9.85 Å and 10.97 Å between the side chain and closest agonist atoms. D) Thr66Ile changes this atomic distance to 6.34 Å and induces unfavourable interactions. E) Val129 at atomic distances of 5.89 Å and 7.56 Å to the closest agonist atoms. F) Val129M mutation indices a flip of BYI08346 and closest agonist atoms are at atomic distances of 2.01 Å and 3.04 Å, respectively.

for the *D. magna* EcR (Fig. 6). Approximately the same increase was also observed for the Met58Ile mutant. None of these amino acids interact directly with BYI08346 and BYI06839 and the mutation has only a structural consequence for the LBP conformation itself (Fig. 8).

The mutation Ala133Ile gave an increase of approximately 20%. This was not unexpected, as isoleucine contains one methyl group more than alanine, and thereby introducing less spatial freedom in the LBP that give unfavourable hydrophobic interactions/clashes between the agonist and the receptor. The mutations Asp134Glu and Gln231Asn changed dG by 10–20%, except for BYI06830 where the Asp134 was replaced with a glutamic acid that caused a 30% increase in dG. Independently of which of these amino acids that are present in position 134, the residue seemed to be located too distantly for direct interaction with the non-steroidal ligands.

4. Discussion

We have used homology modelling and dG calculations by the Prime/MM-GBSA method to evaluate the impact of amino acids substitutions within the agonist LBPs of the *D. magna* EcR. The amino acids for substitution were selected based on amino acid sequence alignments of LBDs of EcRs with known 3D structure and sequences with available agonist binding data. In that way we can also predict the impact of EcR agonist binding in other species than *D. magna*.

4.1. Selection of D. magna EcR homology models

Several of the 200 generated homology models were evaluated to be sufficiently accurate for separating agonists from decoys. On the basis of this evaluation, one model per template was selected for mutational and docking studies. The AUC and BEDROCK scores of these models indicated that the modelling approach provided high quality *D. magna* EcR models. The top ranked models generated for steroidal agonists (Supplementary Fig. 3) gave an AUC of 0.98, which indicates that the model will identify steroidal agonist over the decoy molecules in the docking process with an accuracy of 98%. The corresponding value for the highest scoring model binding non-steroidal agonists was 100%. This clearly shows that we have constructed highly accurate predictive models for docking of steroidal and non-steroidal agonists. A semi-flexible docking protocol was performed where the receptor structure was kept rigid and agonists flexible. Enhanced sampling of the agonists was used to increase the conformational space of the receptor-agonist interactions, which is crucial for increasing the accuracy in the prediction of poses and dG values of the agonists [39]. Alternatively, multiple receptor models could have been used to further increase the conformational space of the receptor-agonist complex, but since the purpose of the study was to investigate the energy contribution by species-specific amino acids in the LBP, it was not considered necessary. The MM-GBSA calculations encounter the entire pocket during calculations, and not only the residues directly involved in binding.

4.2. Analyses of X-ray structures

The LBP of both steroidal and non-steroidal agonists are highly conserved between the EcRs (Supplementary Figs. 1 and 2), and the pattern of agonist interactions are also similar. The X-ray structures show that three amino acids (Glu23, Thr59 and Ala114) form hydrogen bonds with all steroidal agonists. Thr59 and Ala114 are conserved in all EcRs of the present study and were therefore not subjected to mutations. In the *D. magna* EcR, Glu23 is mutated to an aspartic acid (Table 3). Aspartic acid and glutamic acid differ only by a carbon atom in the side chain and have similar physicochemical properties, indicating that the mutation should not significantly affect agonist binding. This was also supported by the MM-GBSA calculations (Fig. 4).

Investigation of the non-steroidal LBP showed that Thr59 and Tyr124 were interacting with the agonists in all available X-ray crystal structures. Thr59 is located in the overlapping part of the steroidal and non-steroidal LBP, is conserved in all the investigated sequences, and participates in agonist interactions independent of co-crystalized agonist. On the basis of this finding, it is likely that this residue is important in facilitating agonist binding to EcRs.

4.3. Prime/MM-GBSA calculations

The dG values calculated by the Prime/MM-GBSA approach of the Schrödinger suit does not encounter explicit water molecules or full conformational entropy and must be considered as approximations of the binding free energy [40]. The dG values should therefore be used for a relative ranking. Relative ranking has been found to correlate well with ranking based on experimental binding affinity [41,42]. Most often, the calculated absolute values are therefore not in direct agreement with experimental binding affinities, which is also shown in the present study where the dG values (Figs. 4 and 6) are heavily overestimated compared with free energy of binding from experimental studies. The dissociation constants (K_i) of Pon A for EcR from *L. cuprina*, *M. persicae*, *B. Tbaci* and *H. armigera* were in the range of 0.5–58 nM, while the corresponding values for 20E were in the range of 66–290 nM [43]. Based on the Gibbs-Helmholtz equation, an experimental affinity value of 1 nM corresponds to a free energy of binding of approximately −9 kcal/mol, while a value of 1 μM corresponds to approximately −6 kcal/mol. A mutation reducing the affinity from the nM range to the μM range should therefore increase the free energy of binding by approximately 30%, while reducing the affinity from the μM to the mM range would require an increase in free energy by approximately 50%.

4.4. In silico mutational studies

The evaluation of the prediction performance indicated that we have generated high quality models that can be used to study the binding of both steroidal and non-steroidal agonists to the *D. magna* EcR. The models are also in a quality to be used for *in silico* mutagenesis in order to study the differences in EcR agonist binding between *D. magna* and other species.

The investigated sequences were highly conserved between species. The lowest identity between sequences was 67%, but more than 70% for most of the sequences (Supporting material, Figs. S2 and S3). The LBP consists mainly of non-polar amino acids with some polar amino acids ensuring hydrogen bonding with hydrophilic groups on the ligands. A similar amino acid distribution in the LBP is described for most nuclear receptors with known X-ray structure [44,45]. Most of the sequences differences between species were quite conserved and should only induce minor changes in the LBP (e.g. mutating between hydrophobic amino acids). Consequently, the largest changes in dG were found when the mutation introduced changes in the physicochemical properties of the LBP, such as the substitution of a polar cysteine in position 100 to nonpolar residues. Disruption of polar or nonpolar interactions in addition to physical changes from small to bulky residues, can drastically change the agonist affinity. Residues found in the steroidal LBP were more conserved across species than residues in the non-steroidal LBP, resulting in smaller mutation-specific changes compared to the non-steroidal LBP in terms of binding free energy.

The *D. magna* EcR is the only among the studied EcRs that has a cysteine at position 100. The residue in this position is involved in both binding of steroidal and non-steroidal agonists (Fig. 3), but is not forming any hydrogen bonds with the interrogated ligands. Interestingly, introduction of a valine in this position changed the dG more than a methionine for the steroidal agonists (Fig. 4), which was directly the opposite for the non-steroidal LBP (Fig. 6). The most predominant change in the steroidal binding pocket was seen for Pon A where mutating the cysteine residue of the *D. magna* sequence to valine resulted in a large decrease in affinity (Fig. 4). A valine in this position enters deeper into the LBP than cysteine and introduce sterical clashes with the steroid (Fig. 5) and thereby destabilize the binding position. In addition, both a valine and a methionine in this position decrease the polarity of the LBP compared with a cysteine. The mutation of Val129 into methionine also reduced the affinity of both steroidal structures for the EcR. A methionine instead of valine in this position induces clashes that destabilize the interactions between the ligand and the LBP. The calculations therefore indicate that species with valine in position 100 (*H. virescens*, *S. littoralis*, *B. mori*) and a methionine in position 129 (*S. littoralis*, *D. melanogaster*, *N. viridula*, *H. virescens*, *B. mori T. castaneum*, *B. tabaci*, *B. ovis*) is less affected by Pon A and 20E binding than *D. magna*. Introduction of valine for threonine in position 132 did not change the dG much for Pon A and only approximately 8% for 20E. In this case, a polar amino acid is changed to a hydrophobic residue, but both of the agonists have their hydrophobic carbon tail positioned against the hydrophobic side chain of valine thus reducing the effect of this mutation.

M58I and T66I are not observed to directly interact with the ligands in the non-steroidal binding pocket, but still these mutations increase the dG value 20% compared with the wild type. This result may be caused by an indirect interactions between the agonist and amino acids in this position by stabilizing the receptor conformation and thereby the ligand pose. When Val129 is exchanged with methionine, BYI06830 flips and positions the aromatic ring towards this amino acid instead of the bulky methyl groups (Fig. 7). This flip seems more favourable for hydrophobic interactions with the pocket since BYI06830 interacts stronger than BYI08346 with the mutant. The methionine perturbs deeper into the LBP than valine and hence destabilize the interactions.

The amino acid sequence of the EcR is highly conserved, but species-specific differences exist and contribute to taxon-specific binding selectivity. In the present study we have used *in silico* methods to study the affinity of EcR agonists across species. In that way, we have been able to predict the species transferability of agonist binding to EcR across species. Largest changes in dG compared with *D. magna* were seen for mutations of Cys100 both for steroids and non-steroids, but also mutations in position 129 contribute to differences between species.

4.5. Use of homology models for predicting EcR agonists, molecular targets and susceptible species

The binding of ecdysteroid-mimicking EDCs to the EcRs has been identified as the molecular initiating event (MIE) of several toxicity pathways leading to molting disruption in arthropods [13], and a dedicated AOP has been developed and submitted to the AOPWiki (https://aopwiki.org/aops/4). Although the taxonomic and chemical applicability domains of this AOP has not been fully defined, the *in silico* methods described herein may facilitate the development of computational models for EcR agonist binding, identify the crucial amino acid for ligand interactions with the LBP and predict species-specific differences in EcR binding specificities, thus expanding both the chemical and taxonomic applicability domains of the AOPs. The model accuracy and speed of computation are ideally suited for more pragmatic approaches such as high-throughput screening of chemical inventories to identify active compounds, definition of the chemical applicability domain of an AOPs, and aid prioritising the most potent EcR binders for more thorough experimental testing [14,15]. The detailed knowledge generated on key amino residues in the EcR ligand-LBD interaction may support defining the taxonomic applicability domain of an AOP and thus form the basis for identifying species likely affected by EcR agonists across a broad set of taxonomic groups [46]. It is envisioned that combinations of *in silico* approaches, as demonstrated herein, and in vitro and in vivo experimental approaches would lend them self useful for consolidating and expanding AOPs, provide building blocks for fit-for-purpose IATA approaches and support hazards assessments of EcR-

mediated endocrine disruption in arthropods [17,20].

5. Conclusions

The present study applied a set of computational methods to characterise the EcR agonist binding pocket in *D. magna*, identify amino acids responsible for differences in agonist binding between arthropod species, and predict the binding affinities of both endogenous and exogenous ligands to the *D. magna* EcR. The multiple sequence alignment and structural analyses clearly showed that the steroidal and non-steroidal LBP are only partly overlapping, and that the steroidal LBP appear to be more conserved than the LBP for non-steroidal agonists. Thr59 is present in both pockets and is conserved across all investigated species. Both Thr59 and Cys100 are present both in the steroidal and non-steroidal LBP, where *in silico* mutations of Cys100 were predicted to cause the largest change to ligand binding and thus were considered the most important determinant for binding differences among species. In addition, sequence variations in position 129 was considered to contribute to large variations in binding affinity across species, where species with a methionine or a valine in position 100 and methionine in position 129 should have lower affinity towards agonists of both steroidal and non-steroidal nature, than species with cysteine and valine at these positions, respectively. Other determinants for species differences are Thr132 for steroidal agonists and Asp134 for non-steroidal agonists. The model evaluation and analysis indicated that we have obtained high quality homology models that can be used to identify potential EcR agonists. The combination of high accuracy and speed of computation makes these models ideal to support defining the chemical and taxonomic applicability domain of AOPs, to form building blocks of IATAs and to support future testing and hazard assessment for EcR-mediated endocrine disruption.

Declaration of Competing Interest

None.

Acknowledgement

The present study was supported by Norwegian Research Council (grant no. 221455 “Adverse Outcome Pathways for Endocrine Disruption in Daphnia magna, a conceptual approach for mechanistically-based Risk assessment”) and by UiT – The Arctic University of Norway. The simulations were performed on resources provided by UNINETT Sigma2 – the National Infrastructure for High Performance Computing and Data Storage in Norway.

Data accessibility

All data can be provided upon request.

Appendix A. Supplementary data

Supplementary data to this article can be found online at https://doi.org/10.1016/j.comtox.2019.100091.

References

[1] T. Colborn, F.S. vom Saal, A.M. Soto, Developmental effects of endocrine-disrupting chemicals in wildlife and humans, Environ. Health Perspect. 101 (5) (1993 Oct) 378–384.
[2] E. Diamanti-Kandarakis, J.-P. Bourguignon, L.C. Giudice, R. Hauser, G.S. Prins, A.M. Soto, et al., Endocrine-disrupting chemicals: an endocrine society scientific statement, Endocr. Rev. 30 (4) (2009) 293–342.
[3] D.M. Fry, Reproductive effects in birds exposed to pesticides and industrial chemicals, Environ. Health Perspect. 103 (Suppl. 7) (1995) 165–171.
[4] M.S. Marty, E.W. Carney, J.C. Rowlands, Endocrine disruption: historical perspectives and its impact on the future of toxicology testing, Toxicol. Sci. 120 (Supplement 1) (2011) S93–S108.
[5] W. Aktar, D. Sengupta, A. Chowdhury, Impact of pesticides use in agriculture: their benefits and hazards, Interdiscip. Toxicol. 2 (1) (2009) 1–12.
[6] Y. Nakagawa, V.C. Henrich, Arthropod nuclear receptors and their role in molting: arthropod nuclear receptors, FEBS J. 276 (21) (2009) 6128–6157.
[7] X. Hu, L. Cherbas, P. Cherbas, Transcription activation by the ecdysone receptor (EcR/USP): identification of activation functions, Mol. Endocrinol. 17 (4) (2003) 716–731.
[8] I.M.L. Billas, T. Iwema, J.-M. Garnier, A. Mitschler, N. Rochel, D. Moras, Structural adaptability in the ligand-binding pocket of the ecdysone hormone receptor, Nature 426 (6962) (2003) 91–96.
[9] I.M.L. Billas, D. Moras, Ligand-Binding Pocket of the Ecdysone Receptor. In: Vitamins & Hormones [Internet]. Elsevier; 2005 [cited 2017 Jul 4]. p. 101–29. Available from: http://linkinghub.elsevier.com/retrieve/pii/S0083672905730041.
[10] M.B. Kumar, D.W. Potter, R.E. Hormann, A. Edwards, C.M. Tice, H.C. Smith, et al., Highly flexible ligand binding pocket of ecdysone receptor: a single amino acid change leads to discrimination between two groups of nonsteroidal ecdysone agonists, J. Biol. Chem. 279 (26) (2004) 27211–27218.
[11] J.M. Beatty, G. Smagghe, T. Ogura, Y. Nakagawa, M. Spindler-Barth, V.C. Henrich, Properties of ecdysteroid receptors from diverse insect species in a heterologous cell culture system – a basis for screening novel insecticidal candidates, FEBS J. 276 (11) (2009) 3087–3098.
[12] A. Stollewerk, The water flea Daphnia – a “new” model system for ecology and evolution? J. Biol. 9 (2) (2010) 21.
[13] Y. Song, D.L. Villeneuve, K. Toyota, T. Iguchi, K.E. Tollefsen, Ecdysone receptor agonism leading to lethal molting disruption in arthropods: review and adverse outcome pathway development, Environ. Sci. Technol. 51 (8) (2017) 4142–4157.
[14] Y. Song, L.M. Evenseth, T. Iguchi, K.E. Tollefsen, Release of chitobiase as an indicator of potential molting disruption in juvenile *Daphnia magna* exposed to the ecdysone receptor agonist 20-hydroxyecdysone, J. Toxicol. Environ. Health A 80 (16–18) (2017) 954–962.
[15] Y. Song, J.T. Rundberget, L.M. Evenseth, L. Xie, T. Gomes, T. Høgåsen, et al., Whole-organism transcriptomic analysis provides mechanistic insight into the acute toxicity of emamectin benzoate in *Daphnia magna*, Environ. Sci. Technol. 50 (21) (2016) 11994–12003.
[16] G.T. Ankley, R.S. Bennett, R.J. Erickson, D.J. Hoff, M.W. Hornung, R.D. Johnson, et al., Adverse outcome pathways: a conceptual framework to support ecotoxicology research and risk assessment, Environ. Toxicol. Chem. 29 (3) (2010) 730–741.
[17] K.A. Fay, D.L. Villeneuve, C.A. LaLone, Y. Song, K.E. Tollefsen, G.T. Ankley, Practical approaches to adverse outcome pathway development and weight-of-evidence evaluation as illustrated by ecotoxicological case studies: AOP development strategies, Environ. Toxicol. Chem. 36 (6) (2017) 1429–1449.
[18] D.L. Villeneuve, D. Crump, N. Garcia-Reyero, M. Hecker, T.H. Hutchinson, C.A. LaLone, et al., Adverse outcome pathway (AOP) development I: strategies and principles, Toxicol. Sci. 142 (2) (2014) 312–320.
[19] D.L. Villeneuve, D. Crump, N. Garcia-Reyero, M. Hecker, T.H. Hutchinson, C.A. LaLone, et al., Adverse outcome pathway development II: best practices, Toxicol. Sci. 142 (2) (2014) 321–330.
[20] K.E. Tollefsen, S. Scholz, M.T. Cronin, S.W. Edwards, J. de Knecht, K. Crofton, et al., Applying adverse outcome pathways (AOPs) to support integrated approaches to testing and assessment (IATA), Regul. Toxicol. Pharm. 70 (3) (2014) 629–640.
[21] R.B. Conolly, G.T. Ankley, W. Cheng, M.L. Mayo, D.H. Miller, E.J. Perkins, et al., Quantitative adverse outcome pathways and their application to predictive toxicology, Environ. Sci. Technol. 51 (8) (2017) 4661–4672.
[22] Prime, Schrödinger, LLC, New York, NY, 2017.
[23] Y. Kato, K. Kobayashi, S. Oda, N. Tatarazako, H. Watanabe, T. Iguchi, Cloning and characterization of the ecdysone receptor and ultraspiracle protein from the water flea Daphnia magna, J. Endocrinol. 193 (1) (2007) 183–194.
[24] M.M. Mysinger, M. Carchia, J.J. Irwin, B.K. Shoichet, Directory of useful decoys, enhanced (DUD-E): better ligands and decoys for better benchmarking, J. Med. Chem. 55 (14) (2012) 6582–6594.
[25] J.-F. Truchon, C.I. Bayly, Evaluating virtual screening methods: good and bad metrics for the “early recognition” problem, J. Chem. Inf. Model. 47 (2) (2007) 488–508.
[26] LigPrep, Schrödinger, LLC, New York, NY, 2017.
[27] The UniProt Consortium, UniProt: the universal protein knowledgebase, Nucl. Acids Res. 45 (D1) (2017) D158–D169.
[28] Protein Preparation Wizard, Schrödinger Release 2017-4: Schrödinger Suite 2017-4.
[29] Epik, Schrödinger, LLC, New York, NY, 2017.
[30] Impact, Schrödinger, LLC, New York, NY, 2017.
[31] R.A. Friesner, R.B. Murphy, M.P. Repasky, L.L. Frye, J.R. Greenwood, T.A. Halgren, et al., Extra precision glide: docking and scoring incorporating a model of hydrophobic enclosure for protein–ligand complexes, J. Med. Chem. 49 (21) (2006) 6177–6196.
[32] Biologics Suite 2018-2, Schrödinger, LLC, New York, NY, 2018.
[33] B. Ren, T.S. Peat, V.A. Streltsov, M. Pollard, R. Fernley, J. Grusovin, et al., Unprecedented conformational flexibility revealed in the ligand-binding domains of the Bovicola ovis ecdysone receptor (EcR) and ultraspiracle (USP) subunits, Acta Crystallogr. D Biol. Crystallogr. 70 (7) (2014) 1954–1964.
[34] J. Li, R. Abel, K. Zhu, Y. Cao, S. Zhao, R.A. Friesner, The VSGB 2.0 model: a next generation energy model for high resolution protein structure modeling, Proteins Struct. Funct. Bioinformatics 79 (10) (2011) 2794–2812, https://doi.org/10.1002/prot.23106.
[35] J.A. Carmichael, M.C. Lawrence, L.D. Graham, P.A. Pilling, V.C. Epa, L. Noyce, et al., The X-ray structure of a hemipteran ecdysone receptor ligand-binding domain: comparison with a lepidopteran ecdysone receptor ligand-binding domain

and implications for insecticide design, J. Biol. Chem. 280 (23) (2005) 22258–22269.
[36] T. Iwema, I.M. Billas, Y. Beck, F. Bonneton, H. Nierengarten, A. Chaumot, et al., Structural and functional characterization of a novel type of ligand-independent RXR-USP receptor, EMBO J. 26 (16) (2007) 3770–3782.
[37] C. Browning, E. Martin, C. Loch, J.-M. Wurtz, D. Moras, R.H. Stote, et al., Critical role of desolvation in the binding of 20-hydroxyecdysone to the ecdysone receptor, J. Biol. Chem. 282 (45) (2007) 32924–32934.
[38] I.M.L. Billas, T. Iwema, J.-M. Garnier, A. Mitschler, N. Rochel, D. Moras, Structural adaptability in the ligand-binding pocket of the ecdysone hormone receptor, Nature 426 (6962) (2003) 91–96.
[39] R.G. Coleman, M. Carchia, T. Sterling, J.J. Irwin, B.K. Shoichet, Ligand pose and orientational sampling in molecular docking, PLoS ONE 8 (10) (2013) e75992Romesberg F, editor.
[40] S. Genheden, U. Ryde, The MM/PBSA and MM/GBSA methods to estimate ligand-binding affinities, Expert Opin. Drug Discov. 10 (5) (2015) 449–461.
[41] J. Du, H. Sun, L. Xi, J. Li, Y. Yang, H. Liu, et al., Molecular modeling study of checkpoint kinase 1 inhibitors by multiple docking strategies and prime/MM-GBSA calculation, J. Comput. Chem. 32 (13) (2011) 2800–2809.
[42] S.K. Tripathi, R.N. Soundarya, P. Singh, S.K. Singh, Comparative analysis of various electrostatic potentials on docking precision against cyclin-dependent kinase 2 protein: a multiple docking approach, Chem. Biol. Drug Des. 85 (2) (2015) 107–118.
[43] I.M.L. Billas, C. Browning, M.C. Lawrence, L.D. Graham, D. Moras, R.J. Hill, The structure and function of ecdysone receptors, in: G. Smagghe (Ed.), Ecdysone: Structures and Functions [Internet]. Dordrecht: Springer Netherlands; 2009 [cited 2018 Jun 9]. p. 335–60. Available from: http://link.springer.com/10.1007/978-1-4020-9112-4_13.
[44] Y. Li, M.H. Lambert, H.E. Xu, Activation of nuclear receptors, Structure 11 (7) (2003) 741–746.
[45] F. Rastinejad, P. Huang, V. Chandra, S. Khorasanizadeh, Understanding nuclear receptor form and function using structural biology, J. Mol. Endocrinol. 51 (3) (2013) T1–T21.
[46] J.A. Doering, S. Lee, K. Kristiansen, L. Evenseth, M.G. Barron, I. Sylte, et al., In silico site-directed mutagenesis informs species-specific predictions of chemical susceptibility derived from the Sequence Alignment to Predict Across Species Susceptibility (SeqAPASS) tool. Toxicol. Sci. [Internet]. 2018 Jul 27 [cited 2018 Sep 4]; Available from: https://academic.oup.com/toxsci/advance-article/doi/10.1093/toxsci/kfy186/5060571.